Journal of
Manufacturing and Materials Processing

MDPI

Article

Investigation of the Influence of Sensorized Tool Holders on Dynamic Properties and Manufacturing Results During Milling

Markus Friedrich [1,*], Benjamin Thorenz [1] and Frank Doepper [1,2]

[1] Chair Manufacturing and Remanufacturing Technology, University of Bayreuth, Universitätsstrasse 30, 95447 Bayreuth, Germany
[2] Fraunhofer Institute for Manufacturing Engineering and Automation IPA, Universitätsstrasse 9, 95447 Bayreuth, Germany
* Correspondence: markus.friedrich@uni-bayreuth.de

Abstract

Monitoring process stability and tool condition is essential for ensuring machining quality and efficiency. This study investigates the influence of sensorized tool holders on dynamic properties and machining results. Three clamping conditions, one conventional and two different sensor-integrated tool holders (equipped with strain gauges or piezoelectric force sensors), are compared. Experimental modal analyses are carried out to determine the frequency-dependent dynamic compliance of the systems. Machining tests using a developed reference workpiece enable the investigation of process forces, wear development, and the surface quality achieved under real conditions. The results show that the dynamic behavior of the tools varies significantly depending on the respective excitation frequency, whereby the different structural properties of the tool holders have a clearly measurable influence on their dynamic properties, particularly near process-relevant excitation frequencies. However, no clear deterioration in terms of process stability or machining performance can be determined. In some cases, the sensorized tool holders can contribute to reduced tool wear and improved process stability. These findings emphasize that sensorized tool holders do not necessarily worsen the machining results and can be applied without negative effects when aligned with the system's modal characteristics.

Keywords: process monitoring; sensorized tool holders; dynamic compliance; machining stability

Academic Editor: Shuting Lei

Received: 18 September 2025
Revised: 16 October 2025
Accepted: 17 October 2025
Published: 19 October 2025

Citation: Friedrich, M.; Thorenz, B.; Doepper, F. Investigation of the Influence of Sensorized Tool Holders on Dynamic Properties and Manufacturing Results During Milling. *J. Manuf. Mater. Process.* **2025**, *9*, 342. https://doi.org/10.3390/jmmp9100342

1. Introduction

Modern production places high demands on manufacturing processes and tools in terms of precision, efficiency, and reliability. In addition to economic challenges, manufacturing processes are also increasingly facing ecological challenges, meaning that sustainability and resource efficiency are becoming ever more important. In order to meet these challenges, continuous monitoring of manufacturing processes and the condition of the tools is essential. There are various approaches to process monitoring and tool condition monitoring. The measurement methods used are divided into direct/indirect and online/offline methods with regard to the measurement principles. Direct approaches are based on the direct acquisition and analysis of data, e.g., via the optical analysis of tools or workpieces, whereas indirect approaches are based on the analysis of auxiliary acquired data that correlates with directly measurable data. Examples of sensors used for indirect approaches include vibration and force sensors. Online methods enable data to be recorded

and analyzed in real-time, whereas with offline methods, data is acquired and analyzed downstream of the process and often in special laboratories. The different approaches have certain implications for applicability in the context of automation and with regard to their accuracy and real-time capability. According to the current state of research, direct approaches usually take place offline, which means real-time capability is not provided. With regard to this real-time capability, online processes are preferable. For this reason, indirect methods are usually chosen, especially in automated systems, although they are more susceptible to noise due to the use of auxiliary signals and the associated longer measuring distance [1,2].

Various research activities have demonstrated the ability to detect tool wear, chatter, or other process anomalies using indirect online methods. The use of force signals is one of the most common and promising, as shown by the large number of research activities and commercially available systems. The force signals have a proven good correlation with the occurrence of process disturbances and can be acquired in various ways [1,3]. One widely used method is the use of sensorized tool holders. Tools are clamped in the sensorized tool holder, which in turn is clamped in the machine spindle. The sensors integrated into the tool holder allow data to be acquired during the machining process. The data is transmitted from the tool holder to a data analysis system in near real time, enabling prompt and comprehensive evaluation. Commercially available systems enable, for example, tool breakage detection or monitoring of tool wear [4,5].

Although sensorized tool holders enable efficient monitoring of the process, their integration also affects the mechanical structure of the spindle–tool–holder combination. In particular, the addition of sensors and transmission hardware, as well as altering the geometry of the tool holder, can alter the mass distribution, stiffness, and damping characteristics, which in turn influence the overall dynamic behavior of the system compared to conventional tool holders. Changes in modal properties may affect process stability, tool wear, and manufacturing results under real machining conditions [6–9].

Although the general impact of tool holder properties on machining dynamics is established in the literature, only limited systematic investigations have quantified how sensor integration specifically affects these dynamic properties. Most existing studies focus on aspects such as signal quality, individual sensor types, or specific monitoring applications, while the broader implications for machining performance remain insufficiently explored [1–3,10,11].

The present work addresses this research gap by systematically investigating the influence of sensorized tool holders on dynamic properties and resulting machining behavior. To this end, two different sensorized tool holder concepts and one conventional tool holder are compared under identical machining conditions. A specially developed reference workpiece is used to ensure standardized and comparable testing. The analysis focuses on four aspects:

- Frequency-dependent dynamic compliance determined by experimental modal analysis;
- Cutting forces and bending moments measured during milling;
- Tool wear progression (by means of the maximum width of the flank wear land $VB_{\max}$) over multiple operations;
- Surface quality of the machined workpieces.

This study provides a comprehensive evaluation that links the structural dynamics of the tool holders to measurable outcomes such as tool wear and surface finish. The findings contribute to a deeper understanding of how sensor integration affects machining behavior and provide guidance for process design and monitoring strategies using sensorized tool holders.

2. Materials and Methods

2.1. Tool and Machine Overview

The tool used was an uncoated solid carbide end mill with a diameter of 10 mm, a number of teeth of 4, a helix angle of 30°, a cutting edge length L_c of 25 mm, and a corner chamfer angle of 45°.

The milling tests were carried out using a 5-axis CNC milling center, type: DMU 50 eVolution, from the manufacturer Deckel Maho Gildemeister (DMG, Bielefeld, Germany) with the Siemens Sinumerik 840D (from the manufacturer Siemens AG, Berlin/Munich, Germany) control system. The machine has a zero point clamping system in the form of an NC high-pressure vice (type 125 from the manufacturer Hoffmann Supply Chain GmbH & Co. (Nuremberg, Germany) KG) and corresponding clamping jaws, which can be used to clamp the workpiece to the machine table. The workpiece is clamped with the maximum clamping force of 40 kN.

Three tool holders were examined in this study. Two of these were sensorized for the measurement of the process forces and torques occurring. Figure 1 provides an overview. In addition, the names used over the course of the paper, e.g., in Section 3, are indicated in the captions of the subfigures. The entire designation is structured as follows: first the designation of the tool holder (configuration 0 represents "Clamping chuck", configuration 1 represents "Sensorized tool holder, type: SPIKE®", configuration 2 represents "Sensorized tool holder, type: RCD (rotating cutting dynamometer)"), followed by the number of the tool used after the underscore (e.g., "_1" stands for tool 1, "_2" for tool 2, etc.).

(**a**) Clamping chuck (conventional, without sensors), name: "configuration 0".

(**b**) Sensorized tool holder, type: SPIKE®, class C, name: "configuration 1".

(**c**) Sensorized tool holder, type: RCD, name: "configuration 2".

Figure 1. Overview of the tool holders examined.

The sensorized tool holder SPIKE®, type C, from the manufacturer pro-micron is equipped with a Multi-Lock chuck, whereas the Wireless RCD from Kistler Instrumente GmbH (Winterthur, Switzerland) is equipped with a collet chuck, type: "ER32". All tool holders are mounted on the spindle using an HSK A63 interface.

2.2. Development of the Reference Workpiece and Process

2.2.1. Approach

The reference workpiece developed and presented in this paper should have a high practical relevance. In addition, further components are to be integrated to characterize the milling process. In summary, the reference workpiece includes

- Real processing cases;
- Stepped plates;
- Line-by-line milling.

Real processing cases were integrated into the reference workpiece to represent machining tasks under real operating conditions. These are based on the examination of real components from companies in different industries, such as tool and die making or general mechanical engineering, as well as expert knowledge from users and tool manufacturers. The machining cases occurring in practice represent changing engagement conditions, infeeds and engagement angles for the milling tool.

As described in Section 2.6, the occurrence of chatter vibrations is problematic, as they cause poor surface quality and dimensional accuracy, heavy wear on the tool and machine, and high noise pollution due to the large vibration amplitudes. In addition, the installed main spindle power of the machine tool cannot be fully utilized, which reduces productivity. This chatter behavior in machining processes is described with so-called stability maps. Following these, in which the course of the limiting axial depth of cut $a_{p;limit}$ is plotted against the spindle speed n, the process stability is to be investigated by integrating stepped plates into the reference workpiece.

Simple line-by-line milling operations are primarily used to quantify the wear behavior. However, the wear behavior was investigated for all operations. In order to be able to show the development of wear over the tool's life, the end mills in clamped condition were removed from the machine tool after each operation and measured in detail.

Another restriction was that all milled surfaces must still be present after the completion of the machining process in order to be able to assess the surface quality afterwards. This is due to the measurement being performed by an external measuring device, which had to be taken into account in the design as well as in the planning of the milling order.

2.2.2. Selection of the Reference Material

When defining a reference workpiece, it is important to select an appropriate material, since the cutting forces are most strongly influenced by the composition of the material, including the base metal and alloy components as well as the microstructure. Paucksch recommends the mechanical parameters of hardness and tensile strength as useful comparative values for the resulting cutting forces [12]. The study of Westermann et al. shows that mainly steels with a tensile strength $<900\ \mathrm{N/mm^2}$ (62%) are machined with solid carbide end mills [13]. A widely used representative of this grade is the unalloyed quenched and tempered steel C45E (material number 1.1191), which has an average tensile strength of 775 MPa. This material is mainly used for components subject to medium stress [14] in general mechanical and plant engineering [15] (e.g., shafts subject to normal stress [16]). Thus, this is considered a suitable reference material and is specified for the reference workpiece defined in this paper.

2.2.3. Construction

Figure 2 shows an isometric view of the developed reference workpiece, which allows a standardized evaluation of vibrations and occurring cutting forces as well as surface quality in metal milling operations. The solid plates used have the dimensions 125 × 125 × 20 mm. The CAD software PTC creo parametric 10.0 was used for the CAD design. The transfer to the machining center was carried out via a CAD-CAM link. Figure 3 shows the individual features, which also correspond to the milling order.

2.2.4. Milling Order and Cutting Parameters

As described in Section 2.2.1, in addition to integrating real processing cases, stepped plates, and line-by-line milling, care had to be taken in planning the milling order to preserve essential elements of the surface after machining in order to subsequently measure its quality.

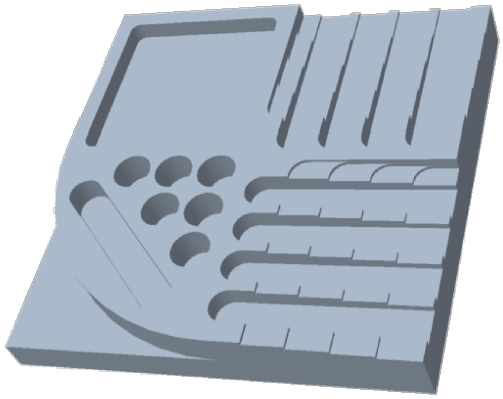

Figure 2. Isometric view of the developed reference workpiece.

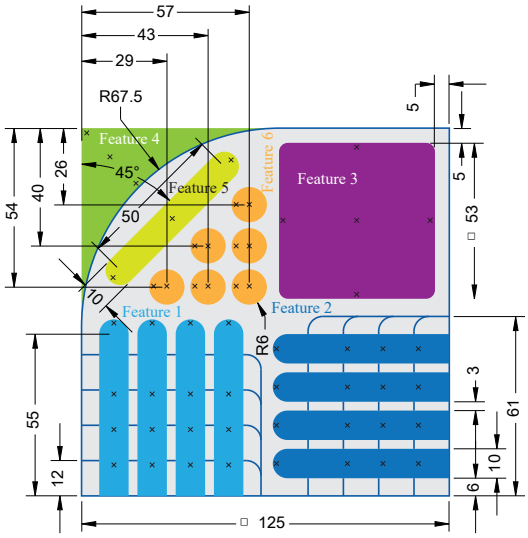

Figure 3. Measuring points for the surface quality assessment. The x mark the points where the measurements are made.

To begin with, the solid plate described was prepared. For this purpose, both the lateral dimensions were milled to size and the drill holes for fastening to a base plate were machined. After this step, the actual machining of the reference workpiece took place.

The steps were created in preparation. These were designed in such a way that the depth of cut a_p increases in discrete steps up to $\Delta a_p = 5$ mm during subsequent over-milling. As considerable differences in machining occur in practice in both the x and y directions, the step plates were arranged symmetrically to compare the stability of the axis directions so that the respective axis bore the main load.

As can be seen in the Figure 3, this was followed in Feature 1 and 2 by the milling of the radiused slot end. These are milled with two different spindle speeds n at a constant feed per tooth f_z and with two different feeds per tooth f_z at a constant spindle speed n. In addition, the feed rate v_f was also varied. The next step was the machining of the pocket (Feature 3). For this purpose, the solid end mill was dipped to the defined depth with a helix before the pocket was milled out. In Feature 4, a typical practical machining operation was carried out—trimming. During programming, this was designed in such a way that both axes of the plane move synchronously in order to bring out differences there as well. In Feature 5, the closed radiused slot end was machined, which was first dipped with a bevel (30) and then milled flat. The last step (Feature 6) did not involve direct

drilling but was carried out by means of helical plunging ($\varnothing_{helix} > \varnothing_{tool}$)—as is common in the industry.

The milling order can also be taken from Table 1 below, which also contains the parameters selected for the milling tests with the tool described above.

Table 1. Example cutting parameters.

#	Operation	a_e mm	a_p mm	f_z mm/tooth	v_f mm/min	n min^{-1}
1a/2a	Radiused Slot End	10	1–5	0.05	382.0	1910
1b/2b	Radiused Slot End	10	1–5	0.07	534.8	1910
1c/2c	Radiused Slot End	10	1–5	0.05	458.4	2292
1d/2d	Radiused Slot End	10	1–5	0.07	641.8	2292
3	Pocket	3	6	0.0615	469.9	1910
4	Trimming	2	10	0.0625	477.5	1910
5	Closed Radiused Slot End	10	8	0.10	159.0	1590
6	Helical Plunging	1		0.10	159	1590

2.3. Experimental Modal Analysis

In order to investigate the dynamic behavior of the tool and the respective influence of the different clamping configurations, an experimental modal analysis is carried out. With the exception of the clamping configuration, the conditions of the experiments are kept the same and the same tool with the same clamping length is used. An automatic impact hammer of the type SAM1 from the company NV Tech Design GmbH (Steinheim, Germany) is used to excite the tool clamped in the machine. The excitation takes place close to the tip of the tool cutting edge so that an excitation situation as close to reality as possible is created. A high-resolution Laser Doppler Vibrometer (LDV) (type PSV-I-680 QTec from Polytec GmbH (Waldbronn, Germany)) is used to measure the velocity response. The contactless measurement ensures precise measurement of the vibration response without interference from a sensor mass or cabling. A measuring grid consisting of several measuring points is distributed over the tool. The measurement is carried out sequentially, whereby three successful strokes are recorded and averaged for each scan point. This approach ensures that the influence of interfering noise is minimized and insights into the spatial resolution are obtained. Data acquisition is carried out using the software "PSV 10.2 Datenerfassung" and data evaluation using the software "PSV 10.2 Auswertung". The excitation force and the velocity response are measured and the transfer function is computed with the use of the H1 estimation method. The common form of representation is dynamic compliance, so that the frequency response function has to be converted into the corresponding form.

2.4. Force and Bending Moment Measurement

Direct force and bending moment measurements are performed using the integrated sensor capabilities of the two sensorized tool holders for configuration 1 and configuration 2. Between the two sensorized tool holders, the methodology differs regarding the distinct sensor technologies.

For configuration 1, the sensorized tool holder Spike® 1.2, type C , is used. The measurement is based on strain gauge technology and enables the measurement of process-related measures such as bending moments in the x- and y-direction, the torsional moment, and the axial force in the z-direction. A system for wireless data transmission to a receiver unit located outside of the machine is integrated into the tool holder. There are different holders for different measuring ranges. The maximum sampling rate of the system used is 2500 Hz; the measuring range for tension is ±53 kN; for torque, it is ±396 Nm; and for bending, it is ±360 Nm with a resolution up to 16 bit. The software for data acquisition

includes simple options for data processing, such as for compensating for thermal drift, as well as for displaying the results.

For configuration 2, the Kistler Wireless RCD (Rotating Cutting Dynamometer) 9170B tool holder is used. This system integrates piezoelectric sensors for the measurement of cutting forces in the three directions (F_x, F_y, and F_z). This tool holder also has a module for wireless data transmission to a receiver unit located outside the machine. The maximum sampling rate of the system used here is 10,000 Hz and the maximum measuring range for F_x and F_y is $\pm$5000 N; for F_z, it is within $\pm$20,000 N; and for M_z, it is within $\pm$100 Nm with a resolution of 16 bit. The system also has software for data acquisition, which has various options for data processing and visualization.

For both configurations, the raw measurement data is saved in the respective standard file formats and then analyzed using suitable scripts written in the Python 3.12 environment. By analyzing and visualizing the signals in the time and frequency domain, a detailed evaluation of the mechanical loads during machining is made possible and potential instabilities can be detected.

2.5. Wear

Cutting materials are subject to a very complex load spectrum during the machining process, which is characterized by high thermal and mechanical stresses and also favors chemical reactions. These high stresses cause wear on the tool cutting edges. The causes of wear include adhesion, abrasion, tribochemical reactions, and surface disruption [17]. In machining processes, tool wear is a critical factor, which influences productivity, workpiece quality and process stability. Monitoring tool wear is therefore essential to ensure the efficiency of the process and to prevent tool breakage. In the context of this study, the observation of the wear progression is important to assess whether and how the use of the different tool holder configurations influences the mechanical loading conditions at the cutting edge and thus the tool life.

In this study, the measurement and evaluation of tool wear is performed using the edgeControl universal measuring machine from ZOLLER and its software pilot 4.0. After each of the different milling operations shown in Table 1, the tool is removed from the milling machine and measured on the measuring device. The tool remains in the tool holder for this process. Figure 4 shows a photograph of the measuring station and a detailed representation of the measurement results.

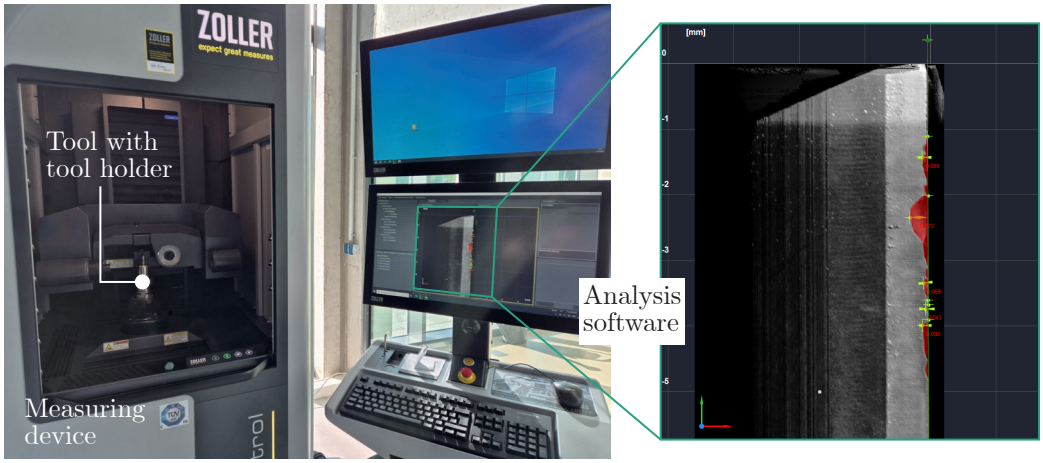

Figure 4. Wear measurement device.

By using a suitable measurement program, the geometry and the condition of each of the four cutting edges of the tool is captured. This is achieved by performing a three-dimensional scan of each individual cutting edge. Using the data from this scan, a de-

spiralized representation of each cutting edge is generated. The de-spiralized representation enables a planar image of the actually spiralized cutting edge and thus a detailed analysis of the signs of wear along the entire cutting edge.

In this study, the maximum width of the flank wear land (VB_{max}) is used as the primary criterion for comparing tool wear between the operations and configurations. This metric is determined by examining the two-dimensional de-spiralized representation of the cutting edge and measuring the maximum extent of wear observed along the entire cutting edge. By using this approach, consistent and reproducible measurements are ensured.

2.6. Surface Quality

The production of an ideal shape or ideally smooth component surfaces is not possible. The surface shape of machined components therefore exhibits position and shape deviations, including surface waviness and surface roughness. These deviations must be reduced to a just permissible level and can be determined by means of different measuring methods and, depending on the filter used, by means of different profiles. According to the DIN EN ISO 4287 standard [18], these are divided into primary profile, roughness profile, and waviness profile. [19] Traditionally, comparative variables such as the arithmetical mean roughness value R_a or the mean roughness depth R_z [18] are used to compare machined component surfaces. In the recent past, there has also been an increase in the use of surface-based measurement methods with values such as the arithmetic mean of the height in relation to the area definition range (S_a) for determining roughness [20–22]. The DIN EN ISO 25178-2 standard [23] takes this surface characterization into account. In addition, the use of functional parameters, such as the core roughness depth R_k [24] or the core height S_k [23], is increasing [25] and has gained industrial acceptance, especially in Europe [26].

The 3D profilometer used in this work, type VR-5000/VR-5200, from the manufacturer Keyence, works according to the fringe light projection method. Due to the possibility of both non-contact and surface-based measurement, area-based characteristic values can be determined, which are expected to be more informative than line values [27]. Figure 5 shows the measurement setup for measuring the surface quality.

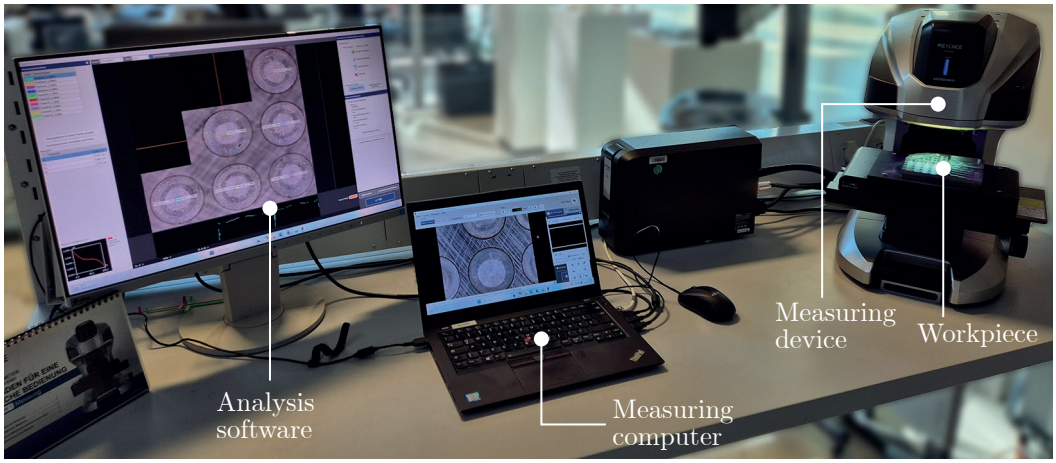

Figure 5. Surface measurement device.

By evaluating the surface quality, far-reaching insights can be gained. The effects of vibrations on the tool or machining center as well as wear on the tool can be seen on the surface.

3. Results and Discussion

3.1. Results of the Experimental Modal Analysis

Figure 6 shows the result of the experimental modal analysis. The H1 transfer functions of the dynamic compliance of the three clamping configurations in the frequency range between 4000 Hz and 8000 Hz are shown. According to the analysis of the scans, the dominant natural bending frequencies of the configurations are located in this frequency range.

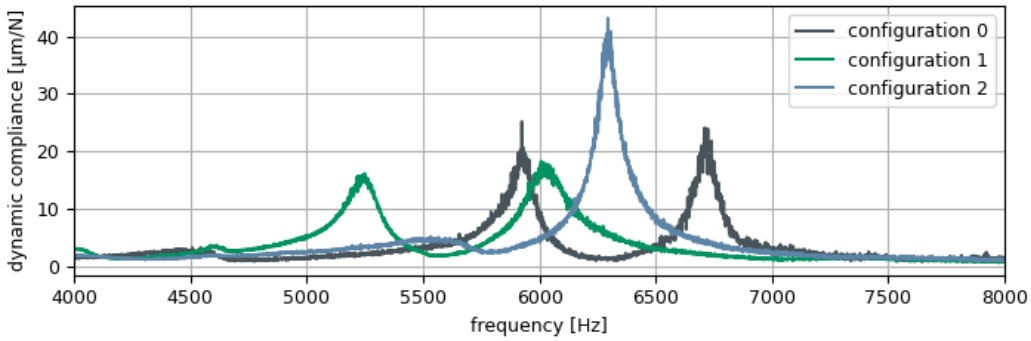

Figure 6. Results of the experimental modal analysis, showing the dynamic compliance in the range of the dominant natural frequencies of the three configurations.

The peaks in the curves represent frequencies at which the system reacts stronger to external excitation, i.e., the tool deflection in a particular direction is larger in terms of µm/N. Within the scope of the investigation, the focus is primarily on the dominant natural bending frequency in the direction of excitation. This is approximately 5950 Hz for configuration 0, approximately 5200 Hz for configuration 1, and approximately 6300 Hz for configuration 2. The amplitudes at the respective natural bending frequencies are approximately 25 µm/N for configuration 0, approximately 16 µm/N for configuration 1, and approximately 42 µm/N for configuration 2. In general, it can be observed that the dynamic compliance is largely similar for all configurations as long as excitation does not take place at a frequency close to the natural frequency. In the case of excitation at natural frequency, the dynamic compliance for configurations 0 and 1 is in a comparable range, although the displacement at configuration 1 is somewhat smaller. This suggests that the damping is slightly better with this configuration. The amplitude of configuration 2 at the corresponding natural frequency is significantly higher than for the other two configurations. However, the dynamic compliance depends significantly on the three influencing factors of mass, damping, and stiffness, and since the respective clamping configurations have different masses and stiffnesses, isolated statements on damping behavior are only possible to a limited extent.

In addition to considering the dynamic compliance in the range of the dominant natural frequencies, analyzing the frequencies of the vibration excitation to be expected during processing is useful. The main excitation frequency during milling corresponds to the tooth passing frequency. Therefore, the dynamic compliance is also analyzed at the frequencies that will occur during the tests. The tooth passing frequency f_{tp} is calculated using the following Equation (1) with the spindle speed n and the number of teeth N_{teeth}:

$$f_{tp} = \frac{n}{60} * N_{teeth} \quad [\text{Hz}] \tag{1}$$

According to Table 1, three different spindle speeds are used in the tests, resulting in tooth passing frequencies of 106.00 Hz, 127.33 Hz, and 152.80 Hz. Figure 7 shows the dynamic compliance in the range between 90 Hz and 200 Hz, with the tooth passing frequencies shown as dashed vertical lines. It can be seen that the amplitudes of the

different configurations differ at the relevant frequencies. Table 2 shows the amplitudes at the frequencies that occur in the process. The differences between configurations 1 and 2 in relation to configuration 0 are shown in brackets.

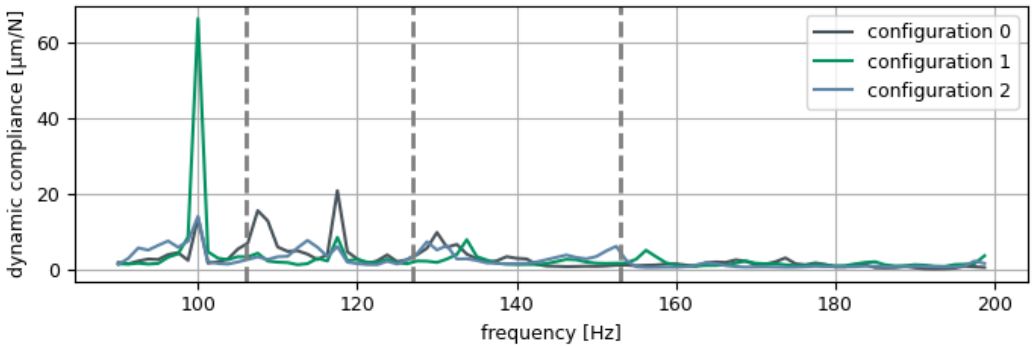

Figure 7. Results of the experimental modal analysis, showing the dynamic compliance in the range of the tooth passing frequencies (vertical dashed lines).

Table 2. Amplitudes occurring in the process at the respective frequencies.

Operations	Frequency Hz	Configuration 0 µm/N	Configuration 1 µm/N	Configuration 2 µm/N
5/6	106.00	6.60	3.30 (−50.09%)	2.46 (−62.77%)
1a/1b/2a/2b/3/4	127.33	3.67	2.09 (−42.96%)	3.92 (+6.62%)
1c/1d/2c/2d	152.80	1.07	1.62 (+50.89%)	5.20 (+385.17%)

The values shown in Table 2 show that the dynamic compliance of configuration 0 is highest for operations 5 and 6. It can therefore be concluded that the process is the most unstable in comparison with these operations. The values for configurations 1 and 2 are approximately 50% and approximately 63% lower, respectively. For the operations in which the tooth passing frequency is 127.33 Hz, the dynamic compliance of configurations 0 and 2 is at a similar level with values of 3.67 µm/N and 3.92 µm/N, respectively. At this frequency, configuration 1 has a dynamic compliance that is approximately 43% lower than that of configuration 0. The lowest dynamic compliance for configuration 0 and configuration 1 is achieved for the operations with a tooth passing frequency of 152.8 Hz. The value for configuration 2 is significantly higher than the values for the other configurations, with an increase of over 385% compared to configuration 0. For the frequencies relevant to machining, configuration 1 shows a rather favorable dynamic behavior overall. Configuration 2 has an advantageous effect at the lower frequencies, but shows clear disadvantages at the highest frequency. The results make it clear that a frequency-dependent evaluation of the tool holders is necessary. It is clear that the influence cannot be assessed as positive or negative across the board but must be considered in a differentiated manner in the context of the prevailing modal properties and the machining parameters. However, with slight deviations in the frequency or spindle speed, which can occur to a certain extent during real machining, the amplitudes of the different configurations sometimes deviate greatly from each other. Under certain circumstances, this influence can lead to chatter and thus to poor machining results or accelerated wear of the tool.

3.2. Results of the Force and Bending Moment Measurements

The comparison of the measured forces between the two sensorized tool holders provides insights into how different structural and sensor integration concepts affect the interaction between tool and workpiece. This is relevant for assessing process stability, tool wear behavior, and the applicability of different tool holder systems to process monitor-

ing in industrial practice. When analyzing the results of the force and bending moment measurements, the differences in the measurement approach must be taken into account. As bending moments are output using the tool holder of configuration 1 and forces directly using the tool holder of configuration 2, the signals must be converted for better comparability. The bending moment signals of configuration 1 can be converted into force signals using the equation $F = M_b / L_{lever}$. According to the manufacturer's drawing for the selected type, the respective lever L_{lever} must be calculated using Equation (2) with the values of the effective length L_{eff} and the depth of cut a_p. The constant value of 69 mm is dependent on the fixed axial positioning of the strain gage sensors within the sensorized tool holder, as specified by the manufacturer [28]. (The maximum deviation of the lever is 4.43% for the depths of cut between 1 and 10 mm that occurred during the tests. The varying depths of cut in the case of continuously rising or falling cuts only minimally distort the results of the calculations.)

$$L_{lever} = L_{eff} + 69\ \text{mm} - \frac{1}{2} * a_p \quad [\text{mm}] \tag{2}$$

It should be noted that part of the observed differences in absolute force levels between configurations is caused by the altered mechanical behavior of the respective tool holder. Variations in clamping, stiffness, mass distribution, and damping affect the load transmission path between the cutting edge and the spindle, leading to different effective forces even under identical cutting conditions. Hence, the differences represent real physical effects and influencing factors. Therefore, when analyzing the force signals, the focus is on the relative differences and the respective developments of the force signals of the individual sensorized tool holders throughout a machining process.

Figures 8–12 show excerpts of the force and bending moment measurements for each operation. Within the tool holders, the results are not significantly different across the test series, which is why only one signal per tool holder is shown as an example to provide a better overview.

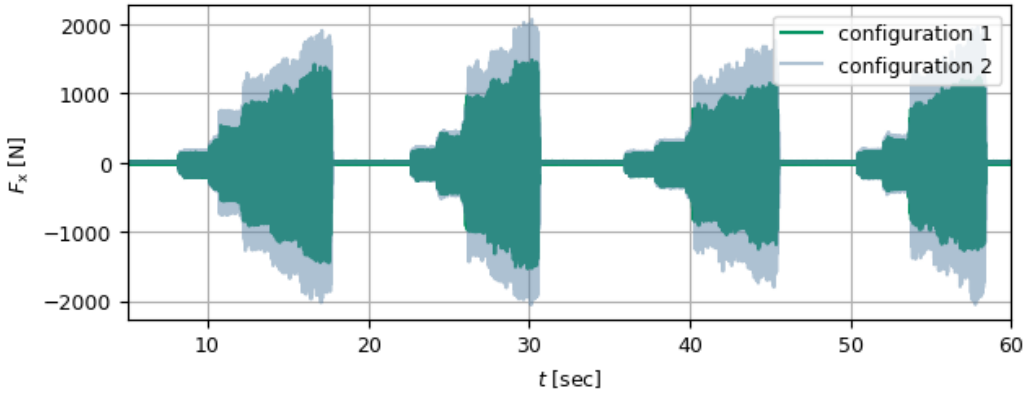

Figure 8. Results of F_x for operation 1.

Figure 8 shows the results for operation 1. The diagram shows four successive machining operations, each of which corresponds to a slot milling operation. Five plateau-shaped steps can be recognized within each slot, which correspond to the steps in increasing depth of cut. The curves show a similar pattern for both configurations: within each slot milling operation, a typical increase in force values can be seen with each additional stage. There are no significant differences in the pattern between the configurations, but there are systematic differences in the force level. For each stage, the signal of configuration 2 is higher than that of configuration 1. The difference is consistently recognizable across all machining operations and is particularly evident at higher depths of cut. Both the

signals for operation 2 and the consideration of the forces in the y-direction provide the same findings.

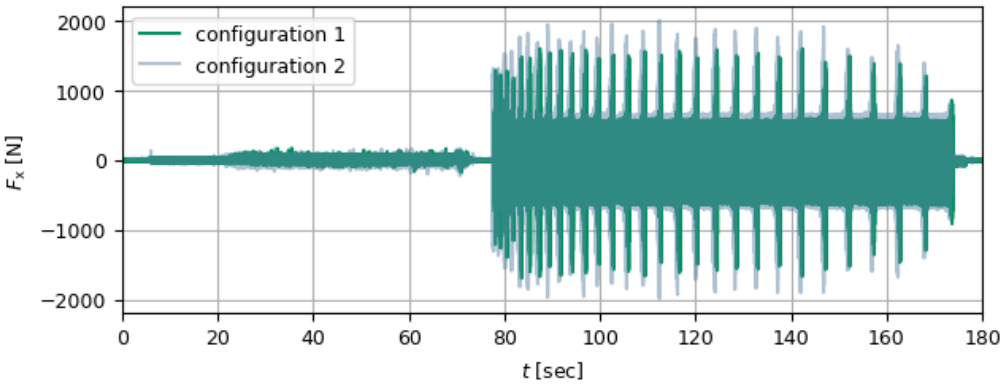

Figure 9. Results of F_x for operation 3.

In Figure 9, the results for operation 3 are shown. The results for the two different configurations are very similar, while the force measured with configuration 2 is approximately 12% higher on average.

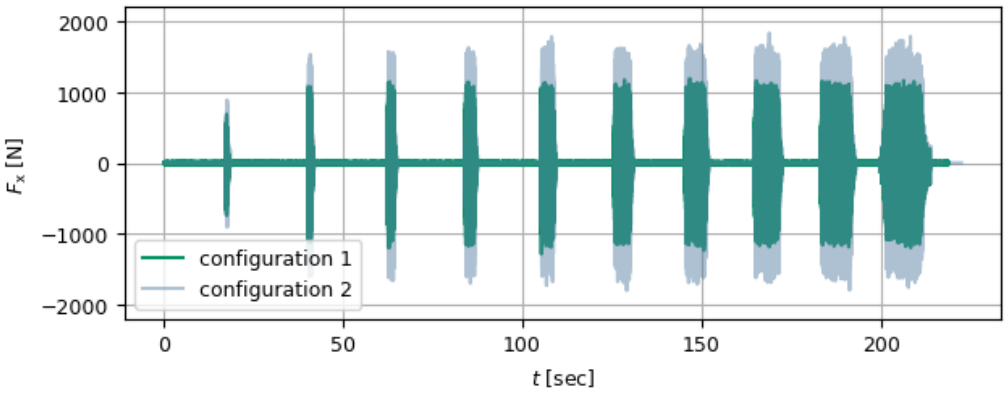

Figure 10. Results of F_x for operation 4.

Figure 10 shows the 10 cuts in operation 4. These become increasingly longer in terms of the time required, whereby the amplitude is largely similar from the second cut onward. The maximum amplitudes are on average 40 % higher for configuration 2 compared to configuration 1.

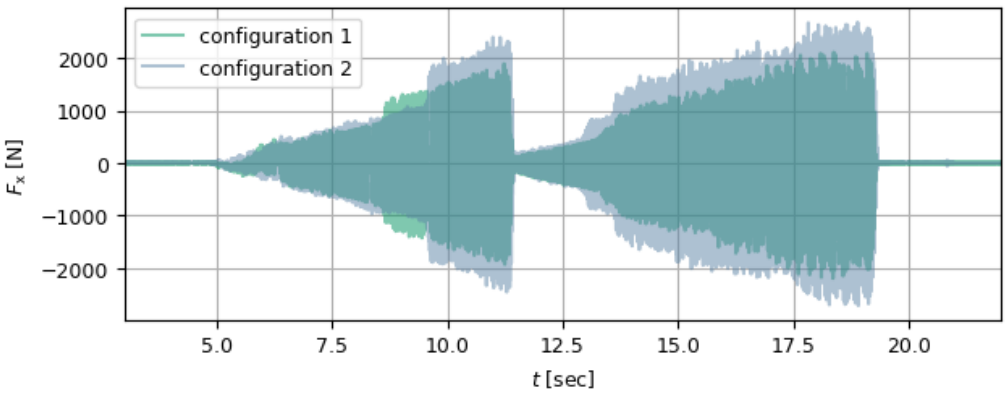

Figure 11. Results of F_x for operation 5.

The forces in the x-direction for operation 5 are shown in Figure 11. The machining operation can be divided into two recognizable parts. The first part shows the plunge with a linear ramp to the final depth of the slot, and the second part shows the machining in the opposite direction and the removal of the remaining part of the ramp to the final depth. For both configurations and for both parts of the machining process, the course of the force shows a continuous increase in each case, whereby this also has a sudden increase for the first part of the machining process. On average, the results of the force measurement in the x-direction are approximately 25 % higher for configuration 2 compared to configuration 1.

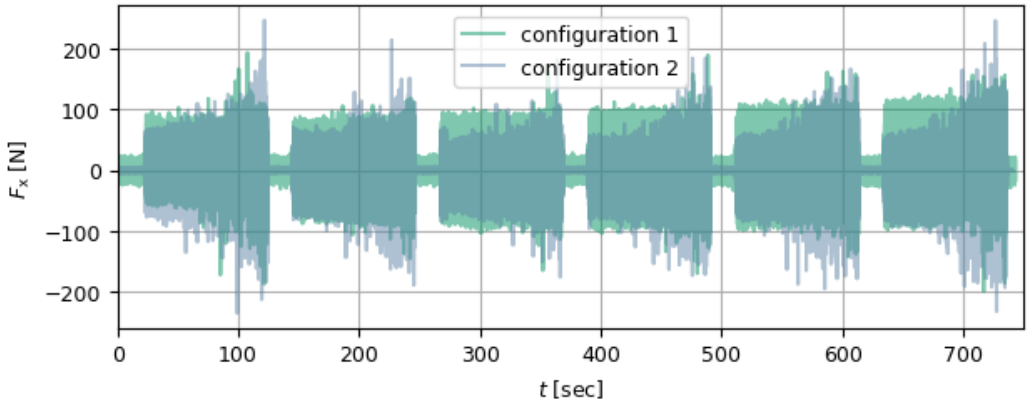

Figure 12. Results of F_x for operation 6.

Figure 12 shows the signals of the helical plunging of operation 6. The signals of the six milling operations have the same basic structure within the respective configuration. Configuration 2 shows a continuous increase in the signal, which is significantly weaker in configuration 1. Configuration 2 tends to measure higher peak forces at the end of each processing step. However, on average, the forces measured with configuration 1 are greater compared to configuration 2 for this feature.

In general, it can be stated that the measured forces for configuration 1 are significantly lower on average in most of the operations compared to configuration 2. The deviation varies depending on the machining process. An exception to this is operation 6, where the average forces for configuration 1 are higher than those measured using configuration 2.

3.3. Results of the Wear Measurement

The results of the wear measurements are shown in Figure 13. The box plot shows the maximum width of the flank wear land in the six different milling operations for the different configurations. The boxes illustrate the distribution of $VB_{\max}$ from three repeated tests per configuration and operation. The median value and the upper and lower outliers are shown.

Across operations, a general trend of increasing wear can be observed with advancing machining. This can be seen particularly clearly with configuration 0 and configuration 1 and is less pronounced with configuration 2. A comparison of the configurations reveals that configuration 1 has the highest average values for operations 1 to 3. From operation 4 onward, there is a massive increase with configuration 0, which means that the highest average values are obtained with this configuration from operation 4 onward. The increase with configuration 1 follows the trend, albeit with a lower gradient. Configuration 2 shows lower values. In particular, the trend across the operations is less steep than with the other configurations. The scattering of the results is highest for configuration 0. Configurations 1 and 2 have lower scatter.

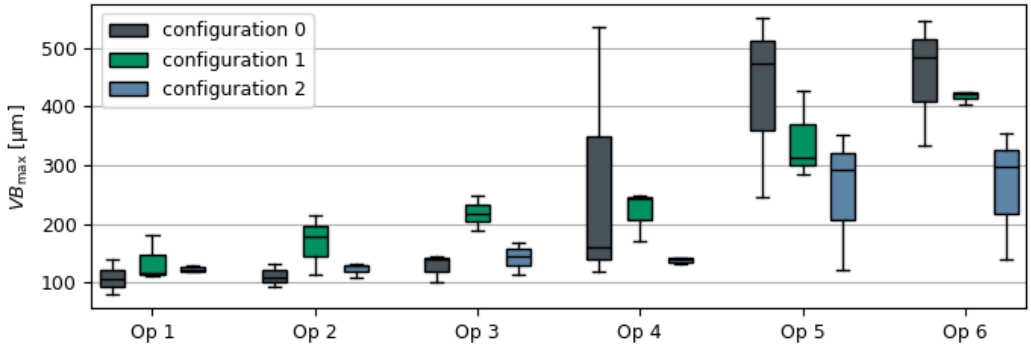

Figure 13. Maximum width of the flank wear land (VB_{max}) per operation for each clamping configuration. The boxplots show data from three repeated tests.

The large scattering of the results for configuration 0 implies poor reproducibility of the test series, which could be an indication of dynamic instability. Such scattering must be regarded as extremely critical with regard to the real use of the tools, as conditions and developments that are as constant as possible are to be preferred with regard to a constant production result. With regard to the maximum width of the flank wear lands at the end of the test series, configuration 0 performs worst. This suggests that the use of sensorized tool holders has a positive influence on wear development during the tests. In terms of tool life, stability and reproducibility, configuration 2 proved to be the best in the tests among the three configurations.

3.4. Results for Surface Quality

Figure 14 shows excerpts of the roughness measurement results. The results show the distribution of the measured surface roughness values S_a in the form of box plots. The first graph shows the results for operation 1, and the second graph shows the results for operations 2 to 6. For operations 1 and 2, the surface roughness values are shown for each milled slot, whereby only the last measuring points at the end of the slot are included in the diagram, as the quality of the surface achieved there is expected to be the worst. For operations 3 to 5, the median of all the measuring points of the corresponding feature per test series was calculated. For operation 6, the median of all edge points was used for each test series.

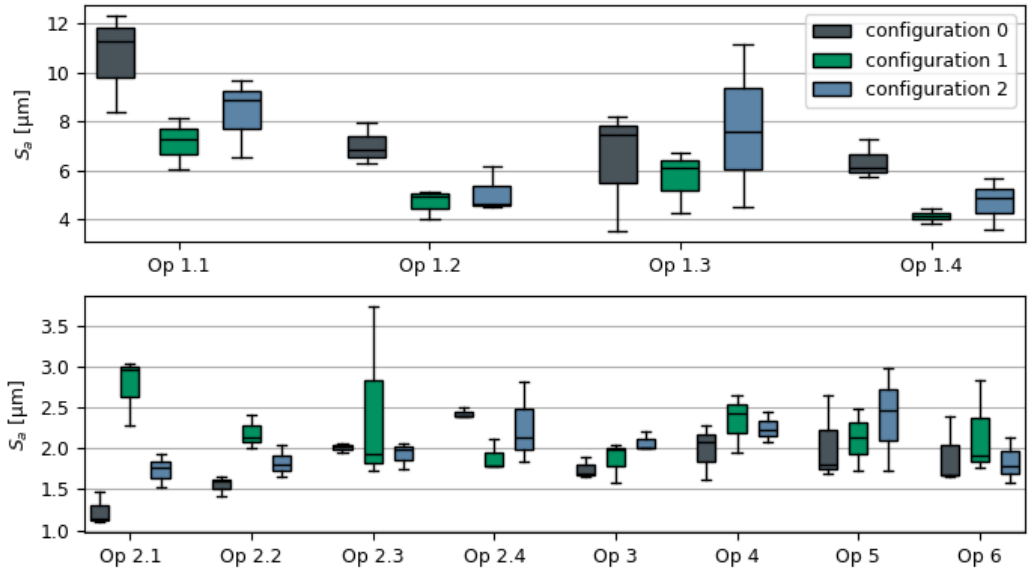

Figure 14. Results of the surface roughness S_a for operation 1 (top) and operations 2 to 6 (bottom).

For operation 1, configuration 0 shows the highest median values and generally a greater scattering than the other two configurations. On average, configuration 1 produces the lowest surface roughness values for this operation. Overall, the surface roughnesses achieved in operation 1 are in a wide range, between approximately 4 µm and 12 µm, and are therefore significantly worse than with all other operations.

In operation 2, configuration 1 delivers the worst results for the first two slots. The results for the other two slots are comparable with each other. Overall, the scatter for operation 2 is lower than for operation 1, with the exception of the third slot for configuration 1, where the scatter is significantly higher than for the other configurations. The roughness values here are in a range between approximately 1 µm and 3 µm and are therefore significantly lower than for operation 1 despite the same machining parameters, albeit in a different coordinate direction.

Operations 3 to 6 tend to achieve lower roughness values of between approximately 1.6 µm to 3 µm. The higher scatter in operations 5 and 6 should be emphasized here, although the values are better overall than in operation 1.

3.5. Discussion

The aim of this study was the investigation of the influence of sensorized tool holders on the dynamic behavior of the system, the resulting machining forces, tool wear progression, and the surface quality of the machined components. A conventional tool holder (configuration 0) was compared with two sensorized tool holders (configurations 1 and 2) from different manufacturers and with different sensor principles. The discussion of the results will lead to differentiated conclusions regarding the advantages and potential drawbacks of using sensorized tool holders.

The experimental modal analysis showed differences in dynamic compliance depending on the configuration. In general, configuration 2 has the highest dynamic compliance at its dominant natural frequency, while the dynamic compliance of configurations 0 and 1 is about 50 % lower. The evaluation at the tooth passing frequencies relevant to actual machining, configuration 1 performed favorably across the majority of the frequencies. At the highest relevant tooth passing frequency, configuration 2 shows the highest increase in dynamic compliance of 385.17 % compared to configuration 0. The frequency-dependent and frequency-specific behavior shows that a general characterization of the dynamic responses of sensorized tool holders as better or worse is not immediately possible. Instead, the dynamic behavior must always be evaluated in the context of the processing parameters.

When measuring the forces and moments occurring, only configurations 1 and 2 could be taken into account. With the exception of operation 6, the consistent pattern was that the amplitudes of configuration 2 were higher. The difference in amplitudes varied depending on the operation but was consistent within the operation, regardless of the test number. In operation 6, the amplitudes of configuration 1 are higher, which may be due to the special characteristics of the helical plunging operation. The systematically lower forces with configuration 1 indicate a potentially favored interaction between tool and workpiece, possibly due to better dynamic properties for the rest of the operations.

In terms of wear development, configuration 2 showed the least wear and the most stable development over time. Configuration 0 showed significantly higher wear from operation 4 onward, coupled with greater scatter. The low reproducibility in configuration 0 suggests unstable cutting conditions, likely due to unfavorable dynamic properties, which can lead to premature tool wear. Configuration 1 showed a moderate behavior, with the values for operations 1 to 3 being the highest on average and from operation 4 onward being between the other two configurations. The scatter of the wear values for configuration 1 is comparatively low. Although configuration 2 had higher cutting forces

in most operations, its dynamic properties suggest a better system response with reduced load fluctuations. This more stable cutting behavior can mitigate wear mechanisms despite higher absolute forces, explaining the observed lower and more consistent wear progression for configuration 2. These results suggest that the use of sensorized tool holders does not necessarily have a negative influence on wear development; in contrast, under certain conditions, it can provide increased stability.

The analysis of the surface roughness achieved showed that the surface quality achieved during the use of sensorized tool holders is mostly the same or only minimally different compared to configuration 0. For operation 1, configuration 1 yielded the best results, despite this operation produced the roughest surfaces overall, indicating unfavorable cutting conditions on this machine in this specific direction. Overall, no definitive preference emerges in terms of surface quality, making it difficult to ascertain a distinctly positive or negative impact from the use of sensorized tool holders.

The results demonstrate that sensorized tool holders do not systematically degrade machining performance. In some configurations, the differing dynamic properties regarding structural mass, stiffness, and damping of the sensorized tool holders can even enhance process behavior.

4. Conclusions

The study investigated the impact of using sensorized tool holders on various aspects of machining performance, including dynamic behavior, process forces, tool wear, and the surface quality of the workpiece. Three different clamping conditions, including one standard clamping chuck and two sensorized tool holders from different manufacturers, were compared in a structured experiment in which standard machining operations were performed using a developed reference workpiece. The key findings of the experiments include the following:

- The dynamic compliance of the tool holder systems differs depending on frequency, with configuration 1 showing more favorable dynamic characteristics across most relevant frequencies.
- The force signals for configuration 1 were consistently lower than those for configuration 2 for most operations, indicating a potentially more stable and efficient cutting process.
- Tool wear progression was most pronounced with the standard clamping chuck, while configuration 2 achieved the most stable wear behavior with minimal scattering.
- The surface roughness measurements showed comparable results for all configurations, whereby the machining direction appears to have a greater influence than the choice of clamping.

In summary, the use of sensorized tool holders does not necessarily have a negative influence on machining performance. Instead, both sensorized configurations can sometimes contribute positively to process stability and tool life. These findings suggest that the integration of sensors and the electronics into tool holder systems not only enables better monitoring of machining processes but can also contribute positively to robustness and process stability.

Thus, from both a technical and a practical standpoint, sensorized tool holders can be a useful solution for indirect online monitoring of machining processes without negatively affecting the results of machining operations.

Author Contributions: Conceptualization, M.F. and B.T.; methodology, M.F. and B.T.; validation, M.F. and B.T.; formal analysis, M.F.; investigation, M.F. and B.T.; resources, B.T.; data curation, M.F.; writing—original draft preparation, M.F. and B.T.; writing—review and editing, M.F., B.T., and F.D.;

visualization, M.F. and B.T.; supervision, F.D.; project administration, F.D. All authors have read and agreed to the published version of the manuscript.

Funding: This research received no external funding.

Data Availability Statement: The data presented in this study is available upon request from the corresponding author.

Conflicts of Interest: The authors declare no conflicts of interest.

Abbreviations

The following abbreviations are used in this manuscript:

EMA	Experimental modal analysis
F_x	Force in x-direction
a_p	Depth of cut
L_{eff}	Effective length
L_{lever}	Lever length
$VB_{\max}$	Maximum width of flank wear land
S_a	Arithmetic mean surface roughness
N_{teeth}	Number of teeth
f_{tp}	Tooth passing frequency
n	Spindle speed

References

1. Nath, C. Integrated Tool Condition Monitoring Systems and Their Applications: A Comprehensive Review. *Procedia Manuf.* **2020**, *48*, 852–863. [CrossRef]
2. Mohamed, A.; Hassan, M.; M'Saoubi, R.; Attia, H. Tool Condition Monitoring for High-Performance Machining Systems—A Review. *Sensors* **2022**, *22*, 2206. [CrossRef] [PubMed]
3. Rehorn, A.; Jiang, J.; Orban, P. State-of-the-art methods and results in tool condition monitoring: A review. *Int. J. Adv. Manuf. Technol.* **2005**, *26*, 693–710. [CrossRef]
4. SPIKE® Monitoring. Available online: https://www.pro-micron.de/en/solutions/spike-monitoring/ (accessed on 9 October 2025).
5. Rotating Dynamometers (RCD) to Measure Cutting Forces Directly on the Cutting Edge. Available online: https://www.kistler.com/DE/en/rotating-dynamometers-rcd-to-measure-cutting-forces-directly-on-the-cutting-edge/C00000578 (accessed on 9 October 2025).
6. Quintana, G.; Ciurana, J. Chatter in machining processes: A review. *Int. J. Mach. Tools Manuf.* **2011**, *51*, 363–376. [CrossRef]
7. Liu, Y.; Liu, Z.; Song, Q.; Wang, B. Development of constrained layer damping toolholder to improve chatter stability in end milling. *Int. J. Mech. Sci.* **2016**, *117*, 299–308. [CrossRef]
8. Xia, Y.; Wan, Y.; Luo, X.; Wang, H.; Gong, N.; Cao, J.; Liu, Z.; Song, Q. Development of a toolholder with high dynamic stiffness for mitigating chatter and improving machining efficiency in face milling. *Mech. Syst. Signal Process.* **2020**, *145*, 106928. [CrossRef]
9. Zhang, P.; Gao, D.; Lu, Y.; Ma, Z.; Wang, X.; Song, X. Cutting tool wear monitoring based on a smart toolholder with embedded force and vibration sensors and an improved residual network. *Measurement* **2022**, *199*, 111520. [CrossRef]
10. An, Q.; Yang, J.; Li, J.; Liu, G.; Chen, M.; Li, C. A State-of-the-art Review on the Intelligent Tool Holders in Machining. *Intell. Sustain. Manuf.* **2024**, *1*, 10002. [CrossRef]
11. Schuster, A.; Otto, A.; Rentzsch, H.; Ihlenfeldt, S. Multi-Sensory Tool Holder for Process Force Monitoring and Chatter Detection in Milling. *Sensors* **2024**, *24*, 5542. [CrossRef] [PubMed]
12. Paucksch, E. *Zerspantechnik: Prozesse, Werkzeuge, Technologien*; Vieweg+Teubner Verlag/GWV Fachverlage: Wiesbaden, Germany, 2008.
13. Westermann, H.-H.; Süchting, M.; Eisinger, E.; Steinhilper, R. *Entwicklungen und Zukunftstrends in der Zerspanung—Ergebnisse der Studie zur "Zerspanung 2020"*; Fraunhofer-Institut für Produktionstechnik und Automatisierung (IPA): Bayreuth, Germany, 2017.
14. GARANT. *Garant ToolScout—Zerspanungshandbuch*; Hoffmann Group: München, Germany, 2014.
15. Bültmann, J.; Hof, J.; Prahl, U. Wärmebehandlung von Stählen. In *Handbuch Stahl*; Bleck, W., Moeller, E., Eds.; Carl Hanser Verlag: München, Germany, 2018.
16. Zimmermann, S.; Klabbers-Heimann, J. Präzisionsstahlrohre im Automobilbau. In *Handbuch Stahl*; Bleck, W., Moeller, E., Eds.; Carl Hanser Verlag: München, Germany, 2018.

17. Klocke, F.; Arft, M. Mechanische und thermische Beanspruchung des Schneidteils. In *Handbuch Spanen*; Heisel, U., Klocke, F., Uhlmann, E., Spur, G., Eds.; Carl Hanser Verlag: München, Germany, 2014.
18. *Deutsche Fassung EN ISO 4287:1998 + AC:2008 + A1:2009*; DIN Deutsches Institut für Normung e.V. EN ISO, D. 4287: Geometrische Produktspezifikation (GPS)—Oberflächenbeschaffenheit: Tastschnittverfahren—Benennungen, Definitionen und Kenngrößen der Oberflächenbeschaffenheit (ISO 4287:1997 + Cor 1:1998 + Cor 2:2005 + Amd 1:2009). Beuth Verlag GmbH: Berlin, Germany, 2010.
19. Degner, W.; Lutze, H.; Smejkal, E. *Spanende Formung: Theorie, Berechnung, Richtwerte*; Carl Hanser Verlag: München, Germany, 2015.
20. Jiang, X.; Scott, P.; Whitehouse, D.; Blunt, L. Paradigm Shifts in Surface Metrology. Part II. The Current Shift. *Proc. R. Soc. A Math. Phys. Eng. Sci.* **2007**, *463*, 2071–2099. [CrossRef]
21. Pehnelt, S.; Osten, W.; Seewig, J. Vergleichende Untersuchung optischer Oberflächenmessgeräte mit einem Chirp-Kalibriernormal. *Tech. Mess.* **2011**, *78*, 457–462. [CrossRef]
22. Leach, R. Introduction to Surface Topography. In *Characterisation of Areal Surface Texture*; Leach, R., Ed.; Springer: Berlin/Heidelberg, Germany, 2013; pp. 1–14.
23. *Deutsche Fassung EN ISO 25178-2: 2012*; DIN Deutsches Institut für Normung e.V. DIN EN ISO 25178-2: Geometrische Produktspezifikation (GPS)—Oberflächenbeschaffenheit: Flächenhaft—Teil 2: Begriffe und Oberflächen-Kenngrößen (ISO 25178-2:2012). Beuth Verlag GmbH: Berlin, Germany, 2012.
24. *Deutsche Fassung EN ISO 13565-2: 1997*; DIN Deutsches Institut für Normung e.V. DIN EN ISO 13565-2: Geometrische Produktspezifikationen (GPS)—Oberflächenbeschaffenheit: Tastschnittverfahren: Oberflächen mit plateauartigen funktionsrelevanten Eigenschaften; Teil 2: Beschreibung der Höhe mittels linearer Darstellung der Materialanteilkurve (ISO 13565-2 : 1996). Beuth Verlag: Berlin, Germany, 1998.
25. Todhunter, L.D.; Leach, R.; Lawes, S.; Blateyron, F. Industrial survey of ISO surface texture parameters. *CIRP J. Manuf. Sci. Technol.* **2017**, *19*, 84–92. [CrossRef]
26. Mathia, T.G.; Pawlus, P.; Wieczorowski, M. Recent trends in surface metrology. *Wear* **2011**, *271*, 494–508. [CrossRef]
27. Eifler, M. *Tendenzen und Herausforderungen in der Geometrischen Produktspezifikation am Beispiel der Rauheitsmesstechnik*; Postdoctoral Qualification; Technische Universität Kaiserslautern: Kaiserslautern, Germany, 2019.
28. pro-micron GmbH. Training Day—Sensory Tool Holder SPIKE®. Available online: https://www.pro-micron.de/en/technology/spike/ (accessed on 3 June 2022).